Hydrophobic Interactions in a Cyanobacterial Plastocyanin−Cytochrome *f* Complex

Peter B. Crowley,[†] Gottfried Otting,[‡] Beatrix G. Schlarb-Ridley,[§] Gerard W. Canters,[†] and Marcellus Ubbink*,[†]

Contribution from the Gorlaeus Laboratories, Leiden Institute of Chemistry, Leiden University, P.O. Box 9502, 2300 RA Leiden, The Netherlands, Department of Medical Biochemistry and Biophysics, Karolinska Institute, S-171 77, Stockholm, Sweden, and Department of Biochemistry and Centre for Molecular Recognition, University of Cambridge, Building O, Downing Site, Cambridge CB2 1QW, U.K.

Received May 23, 2001. Revised Manuscript Received July 19, 2001

Abstract: The complex of the photosynthetic redox partners plastocyanin and cytochrome *f* from the thermophilic cyanobacterium, *Phormidium laminosum*, was investigated by nuclear magnetic resonance (NMR). Chemical-shift perturbation analysis of amide proton and nitrogen nuclei implicates the hydrophobic patch and, to a lesser extent, the "eastern face" of plastocyanin in the complex interface. Intermolecular pseudocontact shifts observed in the complex of cadmium-substituted plastocyanin and ferric cytochrome *f* specifically define the site of interaction to be between the hydrophobic patch of plastocyanin and the heme region of cytochrome *f*. Rigid-body structure calculations using NMR-derived restraints demonstrate that plastocyanin is oriented in a "head-on" fashion, with the long axis of the molecule perpendicular to the heme plane. Remarkably, the structure and affinity of the complex are independent of ionic strength, indicating that there is little electrostatic interaction. Lowering the pH results in limited reorganization of the complex interface, while the binding affinity is unaffected. Therefore, protonation of the exposed copper ligand, His92, plays only a minor role in the complex. In contrast to other electron-transfer complexes, the plastocyanin−cytochrome *f* complex from *P. laminosum* is predominantly controlled by hydrophobic interactions. These findings are discussed in the context of the previously characterized angiosperm complex.

Introduction

Interprotein electron transfer (ET)[1] via transient complex formation requires a balance of specific binding and fast dissociation, thereby enabling both rapid ET and high turnover.[2] How the interactions of two redox proteins are tuned to meet these requirements is fundamental to the understanding of processes such as respiration and photosynthesis. Electrostatic interactions between charged and polar groups and hydrophobic interactions between apolar residues on the protein surfaces provide the driving force behind complex formation. According to the current theory of interprotein ET,[2] long-range electrostatics control the primary recognition step by preorienting the binding sites between partners, thereby increasing the number of productive collisions. In contrast, hydrophobic interactions, which operate over significantly shorter distances, take effect after the initial electrostatic complex has formed and contribute to the specificity required for ET.

During photosynthesis, the mobile type I copper protein plastocyanin (Pc)[3−5] accepts an electron from membrane-bound cytochrome *f* (cyt*f*)[6,7] of the *bf* complex and delivers it to photosystem I (PSI). On the basis of the first crystal structure of Pc (poplar), it was suggested that Pc reactivity toward its partners is mediated by two surface features:[8] the hydrophobic patch, a region of apolar residues surrounding the exposed histidine ligand, and the acidic patches of the "eastern face" (Figure 1A). This hypothesis was initially supported by the demonstration that negatively charged inorganic complexes bind to Pc near the histidine ligand while positively charged complexes bind near the conserved tyrosine residue located in the "eastern face".[10,11] Mutagenesis of residues in the hydrophobic patch and the "eastern face" subsequently revealed the

* To whom correspondence should be addressed. Telephone: +31 71 527 4628. Fax: +31 71 527 4593. E-mail: m.ubbink@chem.leidenuniv.nl.
[†] Leiden University.
[‡] Karolinska Institute.
[§] University of Cambridge.

(1) Abbreviations: ET, electron transfer; Pc, plastocyanin; *PCu*, cuprous plastocyanin; *PCd*, cadmium-substituted plastocyanin; cyt*f*, cytochrome *f*; PSI, photosystem I; NMR, nuclear magnetic resonance; IPTG, isopropylthio-*β*-D-galactoside; NOE, nuclear Overhauser enhancement; HSQC, heteronuclear single-quantum coherence spectroscopy; NOESY, nuclear Overhauser enhancement spectroscopy; TOCSY, total correlated spectroscopy; COSY, correlation spectroscopy.

(2) Bendall, D. S. In *Protein Electron Transfer*; Bendall, D. S., Ed.; Bios Scientific: Oxford, 1996; pp 43−68.
(3) Sykes, A. G. *Struct. Bonding* **1991**, *75*, 175−224.
(4) Gross, E. L. In *Oxygenic Photosynthesis: The Light Reactions*; Ort, D. R., Yocum, C. F., Eds.; Kluwer Academic Publishers: Dordrecht, 1996; pp 413−429.
(5) Sigfridsson, K. *Photosynth. Res.* **1998**, *57*, 1−28.
(6) Gray, J. C. *Photosynth. Res.* **1992**, *34*, 359−374.
(7) Cramer, W. A.; Soriano, G. M.; Ponomarev, M.; Huang, D.; Zhang, H.; Martinez, S. E.; Smith, J. L. *Annu. Rev. Plant Phys.* **1996**, *47*, 477−508.
(8) Colman, P. M.; Freeman, H. C.; Guss, J. M.; Murata, M.; Norris, V. A.; Ramshaw, J. A. M.; Venkatappa M. P. *Nature (London)* **1978**, *272*, 319−324.
(9) Bond, C. S.; Bendall, D. S.; Freeman, H. C.; Guss, J. M.; Howe, C. J.; Wagner, M. J.; Wilce, M. C. J. *Acta Crytallogr.* **1999**, *D55*, 414−421.
(10) Hanford, P. M.; Hill, H. A. O.; Lee, R. W.-K.; Henderson, R. A.; Sykes, A. G. *J. Inorg. Biochem.* **1980**, *13*, 83−88.
(11) Cookson, D. J.; Hayes, M. T.; Wright, P. E. *Biochim. Biophys. Acta* **1980**, *591*, 162−176.

10.1021/ja0112700 CCC: $20.00
Published on Web 10/03/2001

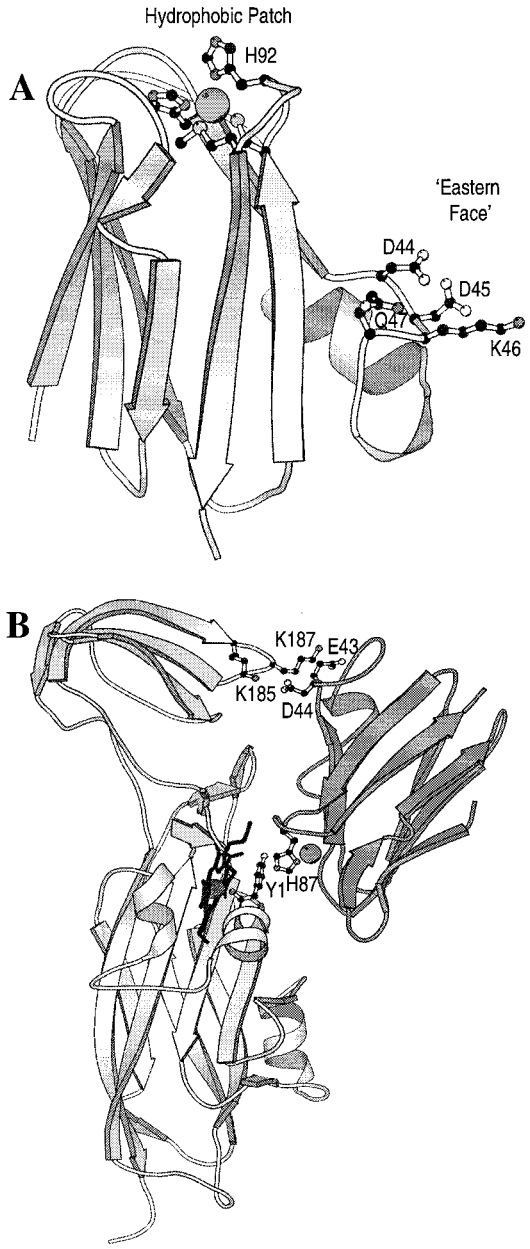

Figure 1. (A) Ribbon diagram of *P. laminosum* Pc[9] with the copper ion indicated as a gray sphere and the type I copper ligands His39, Cys89, His92, and Met97 represented in ball-and-stick. Those residues, corresponding to the lower acidic patch of the "eastern face", are also shown. (B) Ribbon diagram of the complex[17] (PDB entry 2pcf) of spinach Pc[18] (dark gray) and turnip cyt*f*.[19] The copper ligand His87, which protrudes from the hydrophobic patch, makes van der Waals contact with Tyr1, the sixth heme ligand of cyt*f*. D44 and E43 of the lower acidic patch of Pc and K185 and K187 of the small domain of cyt*f* are represented in ball-and-stick.

importance of both surfaces for the in vitro reaction with physiological partners cyt*f*[12−15] and PSI.[14−16]

Once the solution structure of the complex between spinach Pc and the soluble fragment of turnip cyt*f* was determined, it was possible to rationalize how the two binding sites participate to produce an ET complex.[17] It was found that Pc adopts an orientation in which acidic residues of the "eastern face" interact with a ridge of basic residues on the small domain of cyt*f*, while the hydrophobic patch makes contact with hydrophobic residues around the heme (Figure 1B). The structure obtained not only asserted the role of each of the binding sites but also highlighted the importance of electrostatic and hydrophobic interactions in the complex. In addition, the structure provided convincing evidence for an ET path via the exposed ligands of both metal centers, His87 of Pc and Tyr1 of cyt*f*, with a Cu−Fe distance of 10.9 Å. While the structure was in agreement with much of the previous data on Pc−cyt*f* reactivity, the relative importance of the electrostatic and hydrophobic contributions to complex formation and specificity remained unclear.

The character of the "eastern face" is organism dependent, being acidic in Pc isolated from angiosperm (flowering plants)[8,18,20−22] and green-algal[23−25] sources while varying from acidic to basic in cyanobacteria.[9,26−30] In spinach Pc, the "eastern face" is composed of the upper acidic patch (E59, E60, and E61) located proximal to the hydrophobic patch and the lower acidic patch (D42, E43, D44, and E45) remote from the hydrophobic patch.[18] In contrast, the "eastern face" of Pc[9,31] from the thermophilic cyanobacterium *Phormidium laminosum* has fewer charged residues and no distinct recognition site (Figure 1A). The region homologous to the upper acidic patch contains a single charged residue, His61, which lends a basic character to the surface. Arg93 (Q88 in spinach Pc), a conserved residue among the cyanobacterial Pc family, provides additional positive charge in this region of the molecule. The potential binding site of the "eastern face" is thus very different from that of spinach Pc.

Similarly, *P. laminosum* cyt*f*[32,33] is devoid of the ridge of basic residues found in the electrostatically important binding site of angiosperm cyt*f*. Furthermore, the *P. laminosum* protein

(12) Modi, S.; Nordling, M.; Lundberg, L. G.; Hansson, O.; Bendall, D. S. *Biochim. Biophys. Acta* **1992**, *1102*, 85−90.
(13) Kannt, A.; Young, S.; Bendall, D. S. *Biochim. Biophys. Acta*−*Bioenergetics* **1996**, *1277*, 115−126.
(14) Lee, B. H.; Hibino, T.; Takabe, T.; Weisbeek, P. J.; Takabe, T. J. *Biochemistry* **1995**, *34*, 1209−1217.
(15) Hope, A. B. *Biochim. Biophys. Acta*−*Bioenergetics* **2000**, *1456*, 5−26.
(16) Sigfridsson, K. *Photosynth. Res.* **1999**, *59*, 243−247.
(17) Ubbink, M.; Ejdeback, M.; Karlsson, B. G.; Bendall, D. S. *Structure* **1998**, *6*, 323−335.
(18) Xue, Y.; Okvist, M.; Hansson, O.; Young, S. *Protein Sci.* **1998**, *7*, 2099−2105.
(19) Martinez, S. E.; Huang, D.; Szczepaniak, A.; Cramer, W. A.; Smith, J. L. *Structure* **1994**, *2*, 95−105.
(20) Moore, J. M.; Lepre, C. A.; Gippert, G. P.; Chazin, W. J.; Case, D. A.; Wright, P. E. *J. Mol. Biol.* **1991**, *221*, 533−555.
(21) Bagby, S.; Driscoll, P. C.; Harvey, T. S.; Hill, H. A. O. *Biochemistry* **1994**, *33*, 6611−6622.
(22) Sugawara, H.; Inoue, T.; Li, C.; Gotowda, M.; Hibino, T.; Takabe, T.; Kai, Y. *J. Biochem.* **1999**, *125*, 899−903.
(23) Collyer, C. A.; Guss, J. M.; Sugimura, Y.; Yoshizaki, F.; Freeman, H. C. *J. Mol. Biol.* **1990**, *211*, 617−632.
(24) Redinbo, M. R.; Cascio, D.; Choukair, M. K.; Rice, D.; Merchant, S.; Yeates, T. O. *Biochemistry* **1993**, *32*, 10560−10567.
(25) Shibata, N.; Inoue, T.; Nagano, C.; Nishio, N.; Kohzuma, T.; Onodera, K.; Yoshizaki, F.; Sugimura, Y.; Kai, Y. *J. Biol. Chem.* **1999**, *274*, 4225−4230.
(26) Badsberg, U.; Jorgensen, A. M. M.; Gesmar, H.; Led, J. J.; Hammerstad, J. M.; Jespersen, L. L.; Ulstrup, J. *Biochemistry* **1996**, *35*, 7021−7031.
(27) Romero, A.; De la Cerda, B.; Varela, P. F.; Navarro, J. A.; Hervas, M.; De la Rosa, M. A *J. Mol. Biol.* **1998**, *275*, 327−336.
(28) Babu, C. R.; Volkman, B. F.; Bullerjahn, G. S. *Biochemistry* **1999**, *38*, 4988−4995.
(29) Inoue, T.; Sugawara, H.; Hamanaka, S.; Tsukui, H.; Suzuki, E.; Kohzuma, T.; Kai, Y. *Biochemistry* **1999**, *38*, 6063−6069.
(30) Bertini, I.; Ciurli, S.; Dikiy, A.; Fernandez, C. O.; Luchinat, C.; Safarov, N.; Shumilin, S.; Vila, A. J. *J. Am. Chem. Soc.* **2001**, *123*, 2405−2413.
(31) Varley, J. P. A.; Moehrle, J. J.; Manasse, R. S.; Bendall, D. S.; Howe, C. J. *Plant Mol. Biol.* **1995**, *27*, 179−190.
(32) Wagner, M. J.; Packer, J. C. L.; Howe, C. J.; Bendall, D. S. *Biochim. Biophys. Acta*−*Bioenergetics* **1996**, *1276*, 246−252.
(33) Carrell, C. J.; Schlarb, B. G.; Bendall, D. S.; Howe, C. J.; Cramer, W. A.; Smith, J. L. *Biochemistry* **1999**, *38*, 9590−9599.

is strongly acidic at neutral pH, with a net charge of −12 for the soluble fragment compared to −1 for turnip cyt*f*. Given that the charged properties of the *P. laminosum* proteins are very different from those of the angiosperm proteins, the system provides an interesting handle to address the role of electrostatics in transient complex formation. For this reason we studied the complex of Pc and cyt*f* from *P. laminosum* by NMR spectroscopy. It is found that the complex interface involves the hydrophobic patch of Pc and the heme region of cyt*f*. Complex formation in the *P. laminosum* system is largely independent of ionic strength, indicating that the nature of the interaction is primarily hydrophobic. This result is unprecedented in the context of Pc−cyt*f* reactivity, and there is only one previously reported example of a hydrophobic complex between Pc and PSI.[34]

Materials and Methods

Protein Preparation. Uniformly ^{15}N-labeled *P. laminosum PCu* was expressed in *Escherichia coli* BL21(DE3) transformed with the plasmid pET11PC.[35] A 10 mL LB/ampicillin (100 mg/L) preculture grown for 6 h was used to inoculate 1 L of M9 minimal media supplemented with 0.5 g/L $^{15}NH_4Cl$ and 100 μM $Cu(NO_3)_2$. The culture was grown at 37 °C/250 rpm to an OD_{600} of 0.7 before induction by addition of 1 mM IPTG. The temperature was then lowered to 30 °C, and growth was continued for 5 h before harvesting. Isolation and purification of the protein was achieved as described elsewhere.[31] Unlabeled protein was obtained from the same expression system grown on LB medium. Cd^{2+}-substituted Pc was prepared as described previously.[36] The soluble fragment of *P. laminosum* cyt*f* was obtained from *E. coli* MV1190 transformed with both pUC19li5[35] and pEC86[37] grown under semi-anaerobic conditions. A single colony was used to inoculate 1.7 L of LB medium supplemented with ampicillin (100 mg/L) and chloramphenicol (10 mg/L) in a 2 L Erlenmeyer and grown for 20 h at 37 °C/100 rpm before induction by IPTG. The temperature was then lowered to 30 °C and growth continued for a further 36 h. Protein yields up to 15 mg/L were obtained in this manner. This large increase compared with significantly lower yields reported previously[35] was attributed to the plasmid pEC86, which contains the cytochrome *c* maturation cassette.[37]

NMR Samples. Protein solutions were concentrated to the required volume using Millipore Ultrafree centrifugal tubes with a 5 kDa molecular weight cutoff and exchanged into 10 mM potassium phosphate pH 6.0, 10% D_2O, 1.0 mM sodium ascorbate. For the assignment of *PCu*, 2.0 mM ^{15}N-labeled and 1.5 mM and 4.5 mM unlabeled samples were prepared. Protein concentrations were determined by optical spectroscopy using an ϵ_{597} of 4.3 M^{-1} cm^{-1} for the oxidized protein. Cyt*f* samples were prepared to final concentrations ranging from 0.8 to 1.8 mM as determined by ϵ_{556} of 31.5 M^{-1} cm^{-1} for the ferrous form and buffered as described above, while the ferric form was prepared by addition of equimolar amounts of hydrogen peroxide. Complete oxidation was verified by disappearance of the 556 nm band in the UV/vis spectrum. For measurements on the complex, Pc (0.2−1.0 mM) was added to either ferrous or ferric cyt*f*. To study the effects of pH on the complex, a sample of 0.5 mM *PCu* and 1.8 mM ferrous cyt*f* was prepared. The pH was adjusted accordingly by addition of microliter aliquots of 1 M NaOH or 1 M HCl, and spectra were recorded at pH 7.0, 6.0, and 5.0. The effect of ionic strength was investigated at pH 6 by addition of sodium chloride. Spectra were acquired on the *PCu*/ferrous cyt*f* sample at 25, 50, 100, and 200 mM salt concentrations. In all experiments, control measurements were recorded on free Pc under the same conditions. The pH of the NMR samples was measured before and after all experiments.

NMR Spectroscopy. All spectra were acquired at 300 K. For sequence-specific assignment of the backbone resonances of *PCu*, 2D ^{1}H−^{15}N HSQC,[38] 3D ^{1}H−^{15}N NOESY−HSQC[39] (150 ms mixing time), and 3D ^{1}H−^{15}N TOCSY−HSQC (80 ms mixing time) spectra were recorded on a Bruker DMX 600 NMR spectrometer. For assignment of the side-chain protons, 2D homonuclear COSY, NOESY, and TOCSY spectra were recorded on Bruker DRX 500 and Varian Inova 800 NMR spectrometers. PROSA[40] was used for spectral processing, and assignments were performed in XEASY.[41] Measurements on the complex were carried out at 600 MHz ^{1}H NMR frequency. ^{1}H−^{15}N HSQC spectra were recorded with spectral widths of 40.0 ppm (^{15}N) and 17.9 ppm (^{1}H). Analysis of the chemical-shift perturbation with respect to the free protein was performed in XEASY.

The Pseudocontact Effect. Pseudocontact shifts can provide powerful restraints for NMR structure determination,[42−44] while intermolecular pseudocontact shifts have found application in structure determination of protein−protein complexes[17,45,46] and DNA−drug complexes.[47] Metalloproteins often contain metal centers of variable oxidation state, one of which is paramagnetic. In the case of cyt*f*, a low-spin heme protein, the ferrous form (Fe^{2+}) is diamagnetic ($S = 0$) while the ferric form (Fe^{3+}) is paramagnetic ($S = {}^1/_2$). The chemical shift experienced by a nucleus in the presence of the paramagnetic center contains two additional terms with respect to the chemical shift in the diamagnetic protein. Provided that the redox forms of the protein are isostructural, the chemical-shift difference can be attributed solely to the contact effect and the pseudocontact effect:[48−50]

$$\delta_{Ox} = \delta_{Red} + \delta_{CO} + \delta_{PS} \quad (1)$$

where δ_{Ox} and δ_{Red} are the chemical shifts experienced in the oxidized and reduced forms, respectively, and δ_{CO} and δ_{PS} are the contact shift and the pseudocontact shift. The contact shift arises for nuclei which are scalar coupled to the paramagnetic center, and therefore this term can be neglected when considering intermolecular effects. Assuming a metal-centered unpaired electron, the pseudocontact contribution is given by the equation

$$\delta_{PS} = \frac{1}{24\pi r^3}\left\{\left[\chi_{zz} - \frac{1}{2}(\chi_{xx} + \chi_{yy})\right](3\cos^2\theta - 1) + \frac{1}{2}(\chi_{xx} - \chi_{yy})\sin^2\theta\cos 2\phi\right\} \quad (2)$$

where χ_{ii} are the magnetic susceptibility components along the principal axes and r, θ, and ϕ are the polar coordinates of a nucleus relative to these axes.

In this work, eq 2 was treated as described previously for turnip cyt*f*.[17] The χ_{ii} terms for *P. laminosum* cyt*f* are unknown and were replaced by the electronic *g*-values determined for turnip cyt*f*. As the *g*-tensor is essentially axial for an octahedral heme iron, the rhombic

(34) Navarro, J. A.; Hervás, M.; Babu, C. R.; Molina-Heredia, F. P.; Bullerjahn, G. S.; De la Rosa M. A. In *Photosynthesis: Mechanisms and Effects, Vol. III*; Garab, G., Pusztai J., Eds.; Kluwer Academic Publishers: Dordrecht, 1998; pp 1605−1608.
(35) Schlarb, B. G.; Wagner, M. J.; Vijgenboom, E.; Ubbink, M.; Bendall, D. S.; Howe, C. J. *Gene* **1999**, *234*, 275−283.
(36) Ubbink, M.; Lian, L. Y.; Modi, S.; Evans, P. A.; Bendall, D. S. *Eur. J. Biochem.* **1996**, *242*, 132−147.
(37) Schulz, H.; Fabianek, R. A.; Pellicioli, E. C.; Hennecke, H.; Thöny-Meyer, L. *Proc. Natl. Acad. Sci. U.S.A.* **1999**, *96*, 6462−6467.
(38) Andersson, P.; Gsell, B.; Wipf, B.; Senn, H.; Otting, G. *J. Biomol. NMR* **1998**, *11*, 279−288.
(39) Talluri, S.; Wagner, G. *J. Magn. Reson. B* **1996**, *112*, 200−205.
(40) Güntert, P.; Dötsch, V.; Wider, G.; Wüthrich, K. *J. Biomol. NMR* **1992**, *2*, 619−629.
(41) Bartels, Ch.; Xia, T.-H.; Billeter, M.; Güntert, P.; Wüthrich, K. *J. Biomol. NMR* **1995**, *5*, 1−10.
(42) Banci, L.; Bertini, I.; Bren, K. L.; Cremonini, M. A.; Gray, H. B.; Luchinat, C.; Turano, P. *J. Biol. Inorg. Chem.* **1996**, *1*, 117−126.
(43) Allegrozzi, M.; Bertini, I.; Janik, M. B. L.; Lee, Y. M.; Lin, G. H.; Luchinat, C. *J. Am. Chem. Soc.* **2000**, *122*, 4154−4161.
(44) Hus, J. C.; Marion, D.; Blackledge, M. *J. Mol. Biol.* **2000**, *298*, 927−936.
(45) Guiles, R. D.; Sarma, S.; DiGate, R. J.; Banville, D.; Basus, V. J.; Kuntz, I. D.; Waskell, L. *Nature Struct. Biol.* **1996**, *3*, 333−339.
(46) Morelli, X.; Dolla, A.; Czjzek, M.; Nuno Palma, P.; Blasco, F.; Krippahl, L.; Moura, J. J. G.; Guerlesquin, F. *Biochemistry* **2000**, *39*, 2530−2537.
(47) Tu, K.; Gochin, M. *J. Am. Chem. Soc.* **1999**, *121*, 9276−9285.

term in eq 2 is neglected, and substitution results in

$$\delta_{PS} = \frac{\mu_0 {\mu_B}^2 S(S+1)}{72\pi kTr^3}\{2{g_z}^2 - ({g_x}^2 + {g_y}^2)\}(3\cos^2\theta - 1) \quad (3)$$

where μ_0 is the vacuum permeability, μ_B the Bohr magneton, S the spin quantum number, k the Boltzmann constant, and T the temperature. Upon substitution of the numerical values, eq 3 yields

$$\delta_{PS} = \frac{(1.85 \times 10^3)F}{r^3}(3\cos^2\theta - 1) \quad (4)$$

The "bound factor", F, is an additional coefficient which varies between zero and unity and reflects the fraction of Pc in complex with cyt*f*. Only bound Pc can experience chemical-shift changes, and since the complex is in fast exchange, the observed shift is an average of the bound and free contributions. When all Pc is bound, F becomes unity and δ_{PS} reaches a maximum. The best results from the structure calculations were obtained when F was assigned a value of 0.4. The greatly simplified eq 4 highlights the r^{-3} dependence of δ_{PS}. In contrast to the NOE effect, which falls off as r^{-6}, the pseudocontact effect can provide long-range restraints for structure determination. In a complex of two proteins, intermolecular pseudocontact shifts provide distance restraints between nuclei of one protein and the paramagnetic center of the other protein, in this case the heme iron of cyt*f*.

Restraint Classes. Chemical-shift changes experienced by Pc nuclei in the presence of ferrous cyt*f* were attributed to protein binding, and it was assumed that affected nuclei are part of the complex interface. Nuclei, which experience chemical-shift perturbation due to binding ($\Delta\delta_{Bind}$), were identified by subtracting assignments for the free protein from the assignments in the complex:

$$\Delta\delta^i_{Bind} = \delta^i_{pf(II)} - \delta^i_{free} \quad (5)$$

where $\delta^i_{pf(II)}$ and δ^i_{free} are the chemical shifts experienced by nucleus i in the complex with ferrous cyt*f* and in the free protein, respectively. Values of $\Delta\delta_{Bind} \geq 0.08$ (^{1}H) or 0.10 (^{15}N) were translated into interface restraints for the structure calculations.[17] In the presence of ferric cyt*f*, Pc nuclei at the interface experience the effects of protein binding and an additional contribution, the pseudocontact effect. The change in chemical shift ($\Delta\delta_{Ox}$) is given by

$$\Delta\delta_{Ox} = \Delta\delta_{Bind} + \delta_{PS} \quad (6)$$

where δ_{PS} is the pseudocontact shift. Assuming that the $\Delta\delta_{Bind}$ shifts are the same in the complex with ferrous and ferric cyt*f*, the pseudocontact shift was determined by subtracting assignments in the ferrous complex from assignments in the ferric complex:

$$\delta^i_{PS} = \delta^i_{pf(III)} - \delta^i_{pf(II)} \quad (7)$$

where $\delta^i_{pf(III)}$ is the chemical shift experienced by nucleus i in the complex with ferric cyt*f*. The results of this analysis are presented in Table S2 (Supporting Information). Values of $\delta_{PS} \geq 0.08$ (^{1}H) or 0.10 (^{15}N) were used as distance and angle restraints in structure calculations.[17] Target distances for those nuclei were determined using eq 4. Nuclei for which no pseudocontact shifts were observed must lie sufficiently far from the heme iron so as not to experience the paramagnetic effect. These nuclei define a fourth set of restraints, constituting the minimal distance group.

Structure Calculations. To derive the orientation of Pc relative to cyt*f* in the complex, a rigid-body search was performed on the basis of the NMR-derived restraints.[17] To avoid local minima, a restrained rigid-body molecular dynamics (rRB-MD) protocol (X-PLOR version 3.851[51]) was used for this purpose. In this procedure the cyt*f* coordinates[33] are fixed, while Pc is allowed six degrees of freedom (rotational and translational). By exploring the surface of cyt*f*, Pc can find an orientation which fits the NMR restraints. An additional set of restraints was defined to prevent van der Waals collisions between the two molecules. Multiple runs beginning from random orientations show that the convergence is independent of the starting position. No force field was implemented during the calculations; i.e., the energy term was based solely on the restraints. Therefore, the energy has no physical meaning and is better described as an error function. The lowest-error structures are those that fit best with the NMR data. Analysis of the violations and comparison of the back-calculated pseudocontact shifts with the experimental values were done to evaluate the quality of the structures. Figures of the structures were generated using Molscript[52] and Grasp.[53]

Results

Assignment of *P. laminosum PCu*. Complete sequence-specific ^{1}H and ^{15}N resonance assignments were obtained for all backbone amides, except for the resonances of Thr2, Met7, and Ser62 which overlap at pH 6. In addition, the side-chain amides of all asparagine and glutamine residues, the guanidinium side-chain of Arg93, the side-chain NH of Trp31, and the N$-$H$^{\epsilon 2}$ of His39 were assigned. The resonance assignment is also complete for all nonexchangeable protons with the exception of ^{1}H$^{\xi 3}$ of Trp31 and ^{1}H$^{\epsilon 1}$ of His92. Assignments for *Scenedesmus obliquus* Pc[54] proved helpful during the assignment process due to the remarkable similarity found for both ^{1}H$^{\alpha}$ and ^{1}H$^{\beta}$ resonances in regions of high sequence identity. The resonance assignments were deposited at the BMRB (accession code 4080). Throughout this paper the *P. laminosum* Pc residues are numbered according to their own sequence. When necessary, the corresponding spinach numbering and residue type are included in parentheses.

The Complex of *PCu* and Cyt*f*. Addition of 0.5 mM ^{15}N-labeled *PCu* to a 3-fold excess of unlabeled ferrous cyt*f* resulted in a general broadening of the ^{1}H$-^{15}$N HSQC resonances by about 25 Hz, as expected for complex formation (Figure 2). The resonances of the bound and free forms of *PCu* were in fast exchange on the NMR time scale. With the addition of increasing amounts of *PCu*, the shifted resonances moved toward those of the free protein. Due to the relatively weak binding, it was not possible to obtain a complete binding curve. However, it was estimated that the dissociation constant is on the order of 1 mM. Therefore, in the presence of a 3-fold excess of cyt*f*, about half of the *PCu* was bound. Fifteen of 92 resolved backbone amides demonstrated chemical-shift perturbation, with $|\Delta\delta_{Bind}|$ shifts ranging from 0.05 to 0.14 ppm in ^{1}H^N. Significant effects were likewise observed for 37 amide ^{15}N resonances, which shifted by 0.07$-$1.1 ppm. Side-chain amide groups were also affected; in particular, the intensities of the Asn33, Asn34, and Asn40 resonances decreased dramatically. A table of all residues with $|\Delta\delta_{Bind}| \geq 0.05$ (^{1}H^N) or $|\Delta\delta_{Bind}| \geq 0.07$ (^{15}N) is provided as Supporting Information (Table S1).

The chemical-shift changes identify the surface of *PCu* pertinent to the interaction with cyt*f*. Figure 3A shows the location of the residues in the crystal structure of *P. laminosum* Pc,[9] for which $\Delta\delta_{Bind}{}^{15N} \geq 0.1$ ppm was observed. This result highlights the importance of the hydophobic patch surrounding the exposed histidine ligand. The largest $\Delta\delta_{Bind}$ effects were

(48) Kurland, R. J.; McGarvey, B. R. *J. Magn. Reson.* **1970**, *2*, 286$-$301.
(49) Willias, G.; Clayden, N. J.; Moore, G. R.; Williams, R. J. P. *J. Mol. Biol.* **1985**, *183*, 447$-$460.
(50) Bertini, I.; Luchinat, C. *Coord. Chem. Rev.* **1996**, *150*, 1$-$296.
(51) Brunger, A. T. *X-PLOR 3.1 manual*; Yale University Press: New Haven, CT, 1992.
(52) Kraulis, P. J. *J. Appl. Crystallogr.* **1991**, *24*, 946$-$950.
(53) Nicholls, A.; Sharp, K.; Honig, B. *Proteins: Struct., Funct. Genet.* **1991**, *11*, 281$-$296.
(54) Moore, J. M.; Chazin, W. J.; Powls, R.; Wright, P. E. *Biochemistry* **1998**, *27*, 7806$-$7816.

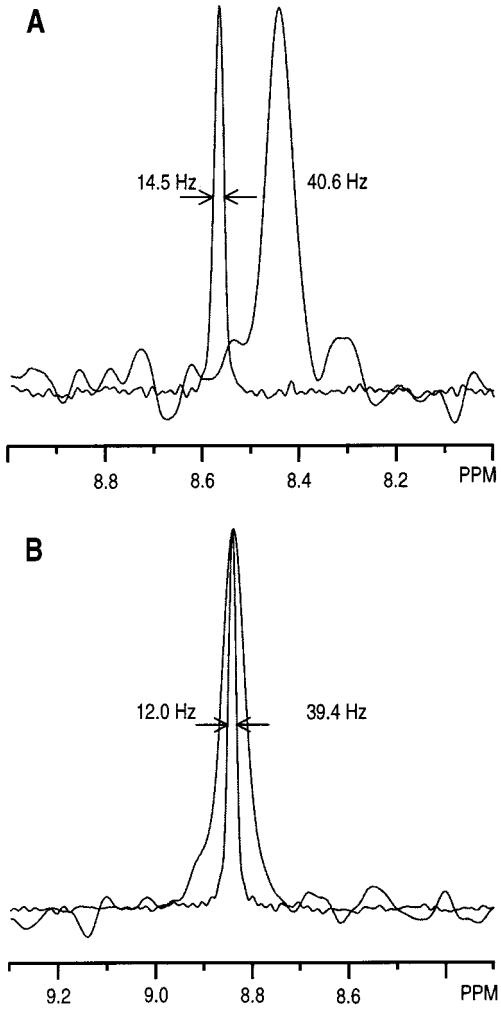

Figure 2. Cross sections along the F_2 dimension through the $^1H^N$ resonances of (A) Leu14 and (B) Lys53 of *P. laminosum PCu*. The resonance of Leu14 shifts by −0.12 ppm in the complex with ferrous cyt*f*, and the line width at half-height increases by 26 Hz. The resonance of Lys53 is not shifted but is still broadened due to the increased rotational correlation time of the complex.

observed for His92 (H87) and neighboring residues Leu13 (S11), Phe66 (N64), and Ala95 (A90). While binding effects occur predominantly in the hydrophobic patch, a few weakly perturbed nuclei are present around the "eastern face" of the molecule. The amide ^{15}N of the buried, copper-coordinating residue His39 was shifted by 0.74 ppm, which is significantly larger than the average shift of 0.19 ppm, suggesting that protein-binding effects are transmitted from the interface to buried residues via the metal site. The plausibility of transmittance effects is further corroborated by the resonance of the imidazole side-chain proton, $^1H^{\epsilon 2}$, of His39 (11.4 ppm), which shifts by 0.08 ppm.

Salt Titration. To determine the importance of ionic strength on the complex of *PCu* and ferrous cyt*f* at pH 6.0, $^1H-^{15}N$ HSQC spectra were recorded over the range of 0−200 mM NaCl. In control measurements on free *PCu*, the backbone amide resonances were unaffected by the presence of salt. A selected spectral region from the overlaid HSQC spectra of free *PCu* and *PCu* in complex with cyt*f* at different salt concentrations is illustrated in Figure 4. No significant changes were observed in the complex with increasing salt concentration. The extent of line broadening was unchanged, and consistent $\Delta\delta_{Bind}$ values were obtained in all experiments, indicating that the amount of complex formed is independent of ionic strength and the complex interface is unaffected. These observations demonstrate that the electrostatic contribution to the complex of *PCu* and ferrous cyt*f* is insignificant at pH 6.0.

pH Effects. At low pH, the exposed histidine ligand in *PCu* becomes protonated and undergoes a conformational change.[55−57] The $^1H-^{15}N$ HSQC spectrum of *PCu* differs markedly between the high- and low-pH forms of the protein. A pK_a of 5.1 ± 0.05 was determined by NMR for the protonation of His92 in *P. laminosum* Pc (Figure 5A). To investigate the effect of the histidine protonation on the complex with cyt*f*, $^1H-^{15}N$ HSQC spectra were recorded on a *PCu*/ferrous cyt*f* sample at pH 7.0, 6.0, and 5.0. The extent of line broadening was similar in all three spectra, indicating that the binding constant for complex formation is independent of pH in this range. Within error (±0.05 ppm), identical $\Delta\delta_{Bind}^{15N}$ shifts were observed for 13 of the 40 affected backbone amides at the different pH values (Figure 5B). At pH 5.0, there is an appreciable decrease in $\Delta\delta_{Bind}^{15N}$ for Leu13, His39, Met65, Ser67, and Ala95, while there is a small increase for Leu64. In addition, the amide ^{15}N of Gly99 is shifted by −0.11 ppm but is unaffected in the complex at higher pH, indicating that there is a pH-dependent rearrangement. The $\Delta\delta_{Bind}^{15N}$ values for both Phe43 and Met97 in the complex at pH 7.0 are intermediate of those at the lower pH values. In the complex at pH 5.0, the amide proton resonance of His92 is exchange-broadened beyond detection, suggesting that the fast exchange limit does not hold for this resonance, which is likely to be strongly shifted between free and bound Pc. If the histidine conformational change promotes dissociation of the product complex (i.e., after ET), there should be up to 50% less complex at pH 5.0, and the magnitude of the $\Delta\delta_{Bind}^{15N}$ shifts should decrease proportionally. More than 30% of the interface residues, however, are unaffected by pH, while those that are pH sensitive do not follow a general trend. These results could be interpreted as evidence that, in the complex at low pH, His92 is not protonated. However, the general appearance of the spectrum of *PCu* in the complex at pH 5.0 more closely resembles that of free *PCu* at pH 5.0 than at pH 7.0. This indicates that His92 is protonated in the complex at low pH and the protonation induces a limited reorganization of the interface, rather than disruption of the complex.

Assignment of *P. laminosum PCd*. Intermolecular pseudocontact shifts between ferric cyt*f* and Pc provide quantitative information on the orientation of Pc in the complex. To identify pseudocontact effects in the complex, it is necessary to perform the appropriate diamagnetic control experiments (eq 7). Redox-inactive Cd^{2+}-substituted Pc was used to exclude ET processes such as the self-exchange[58] or cross reactions. The backbone resonances of *PCd* were assigned by comparison of the assignments for *PCu* with $^1H-^{15}N$ HSQC and homonuclear TOCSY spectra of *PCd*. All 95 observable backbone amides were resolved, as the amide resonances of Thr2, Met7, and Ser62 do not overlap in the Cd^{2+}-substituted protein. Appreciable changes were found in the $^1H-^{15}N$ HSQC spectrum compared with that of *PCu*. In particular, 12 resonances of active site and neighboring residues were shifted by more than 1.0 ppm in ^{15}N. These chemical-shift changes were attributed to the charge difference[36] between Cu^+ and Cd^{2+}. From the available crystal structures of Cu^+-, Cu^{2+}-, and Hg^{2+}-substituted poplar Pc, it is

(55) Katoh, S.; Shiratori, I.; Takamiya, A. *J. Biochem.* **1962**, *51*, 32−40.
(56) Segal, M. G.; Sykes, A. G. *J. Am. Chem. Soc.* **1978**, *100*, 4585−4592.
(57) Guss, J. M.; Harrowell, P. R.; Murata, M.; Norris, V. A.; Freeman, H. C. *J. Mol. Biol.* **1986**, *192*, 361−387.
(58) Marcus, R. A.; Sutin, N. *Biochim. Biophys. Acta* **1985**, *811*, 265−322.

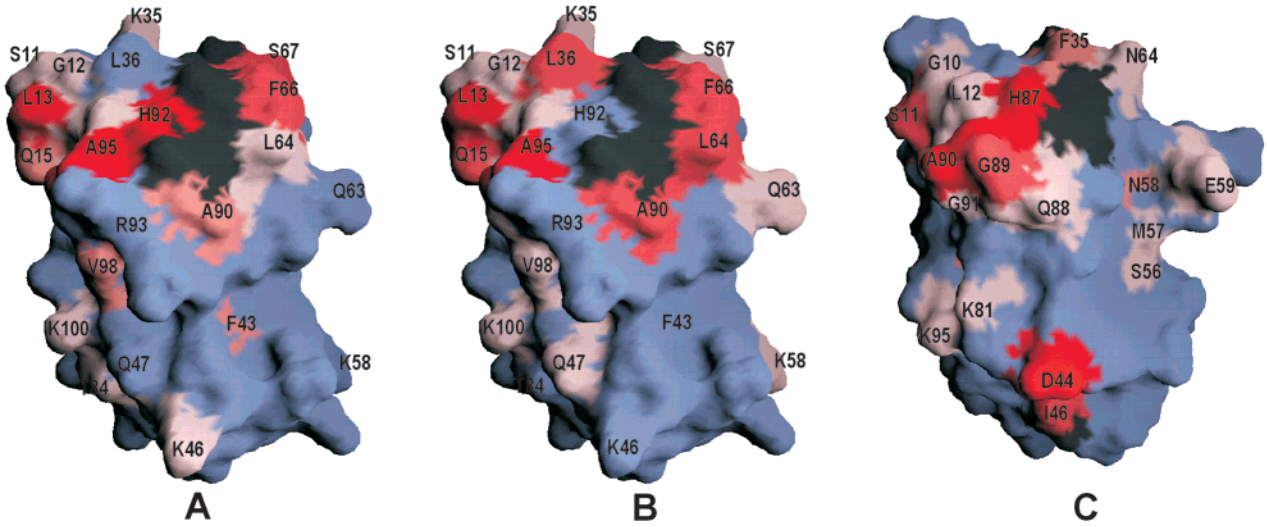

Figure 3. Surface representations of *P. laminosum PCu* (A), *P. laminosum PCd* (B), and spinach *PCd*[17] (C). Residues which experienced chemical shift changes $\Delta\delta_{Bind}{}^{15N}$ in the presence of *P. laminosum* ferrous cyt*f* are color-coded from pale pink (0.1 ppm) to red (≥ 0.5 ppm). Residues with $\Delta\delta_{Bind}{}^{15N} \leq 0.09$ ppm are colored in blue and proline residues in dark gray. Leu14 (L12) has a $\Delta\delta_{Bind}{}^{15N}$ value below the cutoff but was colored pink as it demonstrates one of the largest $\Delta\delta_{Bind}{}^{1H}$ values.

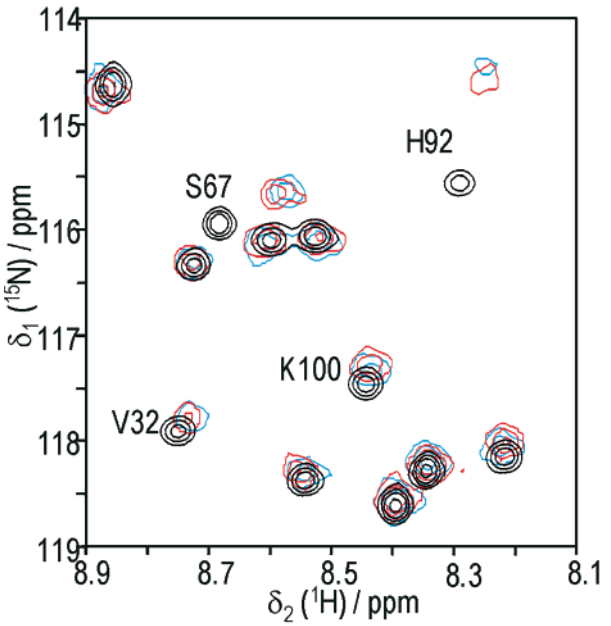

Figure 4. Spectral region from the overlaid $^1H-^{15}N$ HSQC spectra of free *PCu* (black), *PCu* plus a 3-fold excess of ferrous cyt*f* (blue), and *PCu*/cyt*f* with 200 mM NaCl (red).

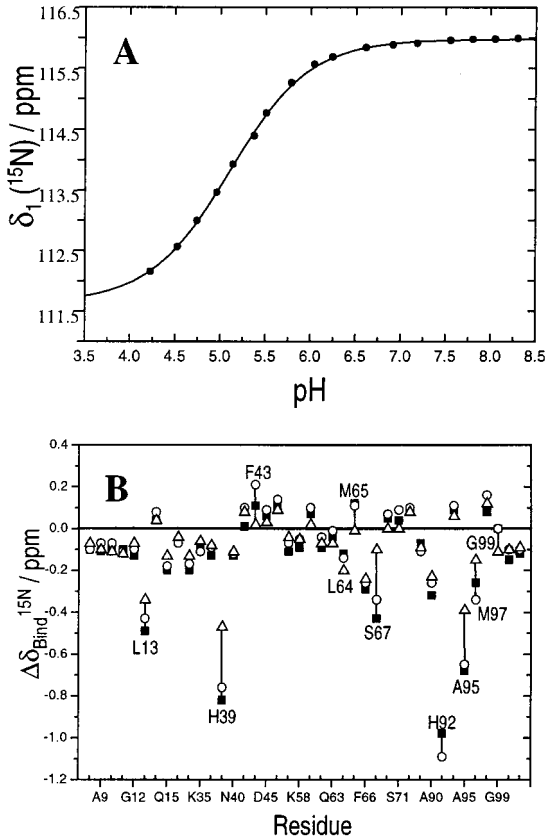

Figure 5. (A) Chemical shift of the amide ^{15}N resonance of His92 as a function of pH. $^1H-^{15}N$ HSQC spectra were recorded on a 1.0 mM sample of *PCu* over the range of pH 4.2−8.3. The data were fitted (three parameters, nonlinear least squares) using the equation $\delta = (K_a\delta_H + [H^+]\delta_L)/(K_a + [H^+])$, where δ_H and δ_L represent the chemical shifts at high and low pH, respectively, yielding a pK_a value of 5.1 ± 0.05 at 300 K. (B) Plot of $\Delta\delta_{Bind}{}^{15N}$ for all 40 affected backbone amide resonances observed in the complex of *PCu* and ferrous cyt*f* at pH 7.0 (■), pH 6.0 (○), and pH 5.0 (△).

evident that the metal exerts a negligible influence on the polypeptide fold.[57,59,60] In these structures, the most significant effect upon metal substitution is a change in side-chain conformation of Pro36 in the hydrophobic patch, while all other side chains seem to remain unaltered.

The Complex of *PCd* and Cyt*f*. As was the case with *PCu*, a general broadening of the $^1H-^{15}N$ HSQC resonances was observed upon addition of ^{15}N enriched *PCd* to a 3-fold excess of ferrous cyt*f*. Sixteen backbone amide resonances demonstrated $|\Delta\delta_{Bind}|$ shifts ranging from 0.05 to 0.16 ppm in $^1H^N$, while 35 experienced shifts from 0.07 to 1.2 ppm in ^{15}N. All residues with $\Delta\delta_{Bind} \geq 0.05$ ($^1H^N$) or $\Delta\delta_{Bind} \geq 0.07$ (^{15}N) are reported in Table S2 (Supporting Information). A surface map of these residues is shown in Figure 3B. Compared with the *PCu* data, identical $\Delta\delta_{Bind}$ values were observed for 40% of the perturbed residues, while variations were found in the immediate vicinity of the metal site and around the "eastern

(59) Guss, J. M.; Freeman, H. C. *J. Mol. Biol.* **1983**, *169*, 521−563.
(60) Church, W. B.; Guss, J. M.; Potter, J. J.; Freeman, H. C. *J. Biol. Chem.* **1986**, *261*, 234−237.

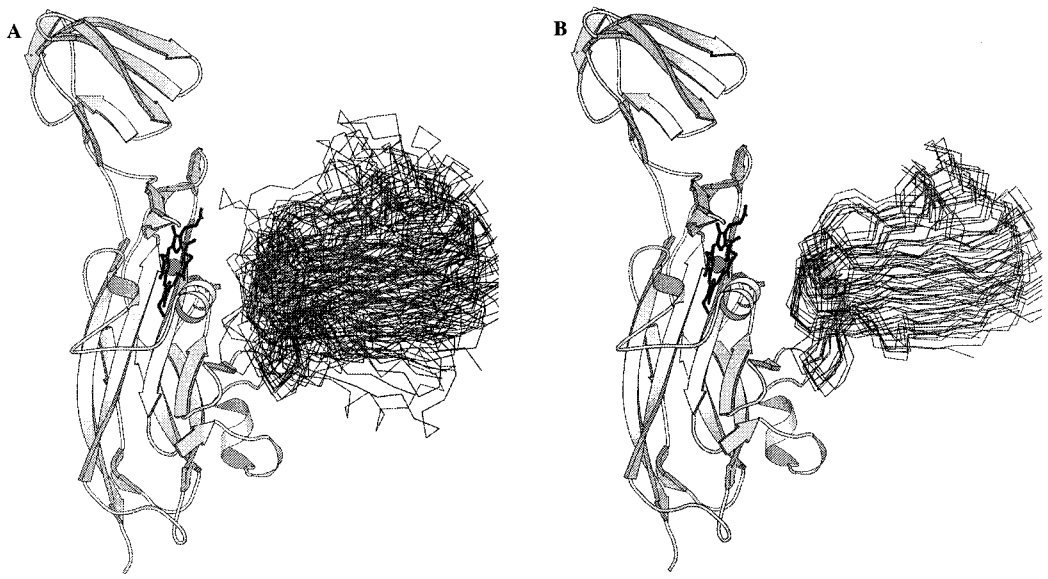

Figure 6. Low-error conformers obtained from X-PLOR calculations. Cyt*f* is represented in ribbon diagram, and Pc is represented as the C^{α} backbone trace. (A) Superposition of 25 orientations of Pc, with the copper centers depicted as gray spheres. (B) Ensemble of 10 conformers representing the predominant structure in the complex.

face". In particular, the amide nitrogen of His92 experiences a 10-fold greater shift in the cuprous protein, indicating that complex formation with ferrous cyt*f* is different for *PCu* than for *PCd*. This illustrates the importance of buried charge in the hydrophobic patch.

In the complex with ferrous cyt*f*, Pc nuclei at the interface experience chemical-shift perturbation due to protein−protein binding. In the presence of ferric cyt*f*, the perturbed nuclei experience the diamagnetic contribution and a paramagnetic contribution manifested as the pseudocontact shift. The size of the latter contribution depends both on the orientation of Pc nuclei relative to the magnetic susceptibility tensor and on the distance from the origin of the paramagnetism. Thus, pseudocontact shifts contain invaluable information about the orientation of Pc relative to cyt*f*. Assuming that the $\Delta\delta_{\mathrm{Bind}}$ shifts are the same in the complex with ferrous and ferric cyt*f*, pseudocontact shifts can be obtained readily from the two experiments (eq 7). Reproducible pseudocontact shifts were determined for a total of 31 residues, located almost exclusively in the hydrophobic patch. For 20 backbone amides $^{1}H^{N}$, δ_{PS} values were in the range 0.05−0.14 ppm, while 29 amide ^{15}N nuclei had δ_{PS} values in the range 0.07−0.9 ppm (Table S2). These results clearly demonstrate that the hydrophobic patch of Pc interacts with the heme region of cyt*f*.

Structure Determination. Chemical-shift perturbation data in combination with the pseudocontact shifts can be used to determine the orientation of Pc in the complex with cyt*f*. From analysis of chemical-shift changes in the presence of ferrous cyt*f*, the hydrophobic patch and, to a lesser extent, the "eastern face" of *PCd* were implicated in the complex interface. Pseudocontact shifts determined in the ferric complex specifically define the site of interaction to be between the hydrophobic patch of Pc and the heme region of cyt*f*. These data provide the basic input for restrained rigid-body calculations in X-PLOR. Beginning from random start configurations, Pc was allowed to explore the surface of cyt*f* in an attempt to satisfy the imposed restraints. In this way, a number of low-error structures were found. The quality of these structures was evaluated on the basis of their violations of the different restraint classes, as defined in the Methods section. Seventy-five percent of the distance restraints derived from the pseudocontact shifts were satisfied in the best structures. Of the 28 restraints, there were on average six violators that differed by more than 0.1 ppm between the experimental and back-calculated pseudocontact shifts. Fewer violations occurred in the minimal distance restraint class, of which between 90 and 95% of the restraints were satisfied. Interface restraints derived from the ferrous complex were the most difficult class to satisfy. This is related to the definition of this class of restraints.[17] Only 50% of the restraints were in agreement with the back-predicted values.

None of the structures obtained were homologous with the angiosperm complex.[17] Using Swiss-PDB Viewer,[61] the *P. laminosum* proteins were aligned with the structure of the angiosperm complex applying the Iterative Magic Fit option to all backbone atoms. Pseudocontact shifts were then back-calculated for this model, yielding a mere 30% agreement with the experimental values. Furthermore, in this orientation, negative pseudocontact shifts were calculated for one-third of the affected nuclei, while only one negative pseudocontact was observed experimentally. When this model was used as a starting configuration for calculations in X-PLOR, Pc moved away from the starting position and low-error structures were found, which were homologous to the structures obtained from random start configurations.

Twenty-five low-error structures obtained from different runs were overlaid for display (Figure 6A). The resulting model has a high degree of variability, but in all cases the hydrophobic patch of Pc makes van der Waals contact with the hydrophobic surface around the heme of cyt*f*, with an average Cu−Fe separation of 15 ± 2 Å. In all cases His92 (H87) makes contact with the highly solvent exposed Phe3 (L3 in turnip cyt*f*). This contact involves the $N^{\epsilon 2}$ of the imidazole ring, which in most conformers stands perpendicular to the aromatic ring of Phe3, while the rings are parallel in some conformers. Within the group of 25 structures, 10 are relatively similar and represent the predominant structure of the complex (Figure 6B). The average pairwise positional root-mean-square deviation[17] (rmsd) of these 10 structures was calculated, using MOLMOL,[62] to be 3.7 Å for the backbone atoms.

(61) Guex, N.; Peitsch, M. C. *Electrophoresis* **1997**, *18*, 2714−2723.
(62) Koradi, R.; Billeter, M.; Wüthrich, K. *J. Mol. Graphics* **1996**, *14*, 51−55.

Discussion

The Complex of Pc and Ferrous Cyt*f*. Reproducible chemical shift changes were observed in the $^1H-^{15}N$ HSQC spectra of both *PCu* and *PCd* in the presence of ferrous cyt*f*. Mapping the chemical-shift changes onto the crystal structure of Pc reveals the complex interface. The largest effects are found in the hydrophobic patch, with fewer effects around the "eastern face" of the molecule. Overall, the maps are similar for both *PCu* and *PCd*, with significant differences, however, for His92 and neighboring residues Leu64 and Leu36. Differences also occur in the "eastern face". This variability, arising from the substitution of Cu^+ by Cd^{2+}, highlights the important role of the metal charge in the complex interface.

Chemical-shift mapping was also applied to the $\Delta\delta_{Bind}{}^{15N}$ shifts observed for spinach *PCd* in complex with turnip cyt*f*[17] (Figure 3C). The surface of the protein involved in the interface is approximately similar in both the cyanobacterial and angiosperm complex, but close inspection of the maps reveals distinct differences between the two systems. Most striking is a ridge of strongly shifted residues, Leu64, Phe66, Ser67, and Ala90, on the hydrophobic patch in *P. laminosum* Pc. The corresponding region of the spinach protein has less hydrophobic character and, with the exception of Asn64, experiences no shifts. (It should be noted that a shift of −0.12 ppm was observed for the side-chain $^1H^\gamma$ of Leu62 in experiments with unlabeled spinach Pc.[63]) Two Leu and two Ala residues in the hydrophobic patch of *P. laminosum* Pc each replace a Gly and Ser in the spinach protein. Of these four, Leu36 (G34) and Ala90 (Ser85) both experience considerable $\Delta\delta_{Bind}{}^{15N}$ effects, while the corresponding residues are unaffected in the spinach protein. On the other hand, residues His87, Gln88, and Gly89 feature on the spinach map, while the corresponding cluster, His92, Arg93, and Gly94, is unaffected in *P. laminosum* (His92 shifts by 0.07 ppm in ^{15}N). The conserved arginine of the cyanobacterial Pcs has been implicated in the reaction with both cyt*f*[64] and PSI,[65] but neither the amide nor the guanidyl side-chain resonances are shifted in the complex.

From this analysis, it is clear that the protein interactions in the *P. laminosum* complex are more hydrophobic in nature than in the angiosperm complex, while the "eastern face" is less important. The "eastern face" of spinach Pc participates in electrostatic interactions with basic residues on cyt*f*, and consequently Asp44 has a very large $\Delta\delta_{Bind}$ value. Such large effects were not observed on the "eastern face" of *P. laminosum* Pc. The relative unimportance of electrostatic interactions in the *P. laminosum* system was further demonstrated by measurements on the complex at different salt concentrations. If there was a dominant electrostatic interaction in the complex, Debye screening of charged groups would tend to decrease the effects observed by NMR. Despite the addition of up to 200 mM NaCl, however, only slight changes were observed, implying that the complex remains intact even at high ionic strength. This observation is in agreement with unpublished results from stopped-flow kinetics.[64]

pH Effects. Protonation of the cuprous site is a typical feature of several subfamilies of the type I copper protein class. At low pH, the exposed histidine ligand, which protrudes from the hydrophobic patch in Pc,[57] amicyanin,[66,67] and pseudoazurin,[68] dissociates from the copper center and becomes protonated. Analysis of the poplar Pc crystal structure at six pH values shows that the imidazole side chain rotates 180° around the $C^\beta-C^\gamma$ bond when no longer constrained to the active site.[57] In addition, the side chain of the neighboring residue, Pro36 (poplar Pc), flips between the C^γ-*exo* and C^γ-*endo* conformations. To compensate for the lost bonding contribution, the cuprous ion falls into the plane of the remaining three ligands, producing a more trigonal site with a concomitant rise in the reduction potential.[69] The functional role of such a pH-induced redox inactivation in a molecule designed for ET has yet to be fully elucidated. It may be envisaged that upon reduction by cyt*f*, in the low-pH limit, the conformational change of His92 and Pro38 acts as a trigger to eject Pc from the complex interface. To test this hypothesis, the complex of *PCu* and ferrous cyt*f* was studied as a function of pH. The results obtained, however, indicate a pH-mediated reorganization of the interface as opposed to disruption of the complex. Recently, Hunter et al.[70] demonstrated that the electron self-exchange[58] rate is slightly higher at pH 5.6 than at pH 6.2 in parsley plastocyanin ($pK_a = 5.7$). This observation was rationalized on the basis that lower pH facilitates protein−protein association by removal of charges in the acidic patch, thus compensating for the expected decrease in k_{ET}. In the complex of *PCu* and cyt*f*, association of the negatively charged proteins could be favored at low pH. However, the electrostatic interaction in the complex was demonstrated to be negligible at pH 6.0, and therefore it can be assumed that the protein association is similarly unaffected by pH.

Structure Determination. Structure calculations based on the NMR data produced an ensemble that gives a clear idea of the orientation of Pc in the complex. However, a single, converged structure was not obtained. This could be interpreted on the basis that the observed pseudocontact shifts do not represent a single orientation, but rather the average of two or more orientations. If these conformers are in fast exchange, the NMR-based method cannot distinguish them. Alternatively, the low convergence might reflect a limitation of the method, as the set of restraints may be insufficient to obtain a precise orientation. Determination of the pseudocontact shifts relies on the assumption that the $\Delta\delta_{Bind}$ shifts are the same in the complex of Pc with both ferrous and ferric cyt*f*. Measurements on the complex between ferrous cyt*f* and either *PCu* or *PCd* indicate, however, that the observable $\Delta\delta_{Bind}$ shifts are dependent on the charge in the hydrophobic patch. Similarly, it can be expected that the charge change upon oxidation of cyt*f* from Fe^{2+} to Fe^{3+} influences the $\Delta\delta_{Bind}$ effects. Furthermore, an approximation of the magnetic susceptibility tensor was used, which could limit the accuracy of the calculations.

A representative structure of the *P. laminosum* complex is illustrated in Figure 7. The orientation of Pc differs considerably from that found in the complex determined for spinach Pc and turnip cyt*f* (Figure 1B). In contrast to the "side-on" orientation found in the angiosperm complex, *P. laminosum* Pc interacts in a "head-on" manner with cyt*f*. In this orientation, the hydrophobic contacts are maximized and the "eastern face" does

(63) Ejdeback, M.; Bergkvist, A.; Karlsson, B. G.; Ubbink, M. *Biochemistry* **2000**, *39*, 5022−5027.
(64) Schlarb-Ridley, B. G. Unpublished results.
(65) Molina-Heredia, F. P.; Hervás, M.; Navarro, J. A.; De la Rosa, M. A. *J. Biol. Chem.* **2001**, *276*, 601−605.
(66) Lommen, A.; Canters, G. W. *J. Biol. Chem.* **1990**, *265*, 2768−2774.
(67) Buning, C.; Canters, G. W.; Comba, P.; Dennison, C.; Jeuken, L.; Melter, M.; Sanders-Loehr, J. *J. Am. Chem. Soc.* **2000**, *122*, 204−211.
(68) Dennison, C.; Kohzuma, T.; McFarlane, W.; Suzuki, S.; Sykes, A. G. *Inorg. Chem.* **1994**, *33*, 3299−3305.
(69) Armstrong, F. A.; Hill, H. A. O.; Oliver, B. N.; Whitford, D. *J. Am. Chem. Soc.* **1985**, *107*, 1473−1476.
(70) Hunter, D. M.; McFarlane, W.; Sykes, A. G.; Dennison, C. *Inorg. Chem.* **2001**, *40*, 354−360.

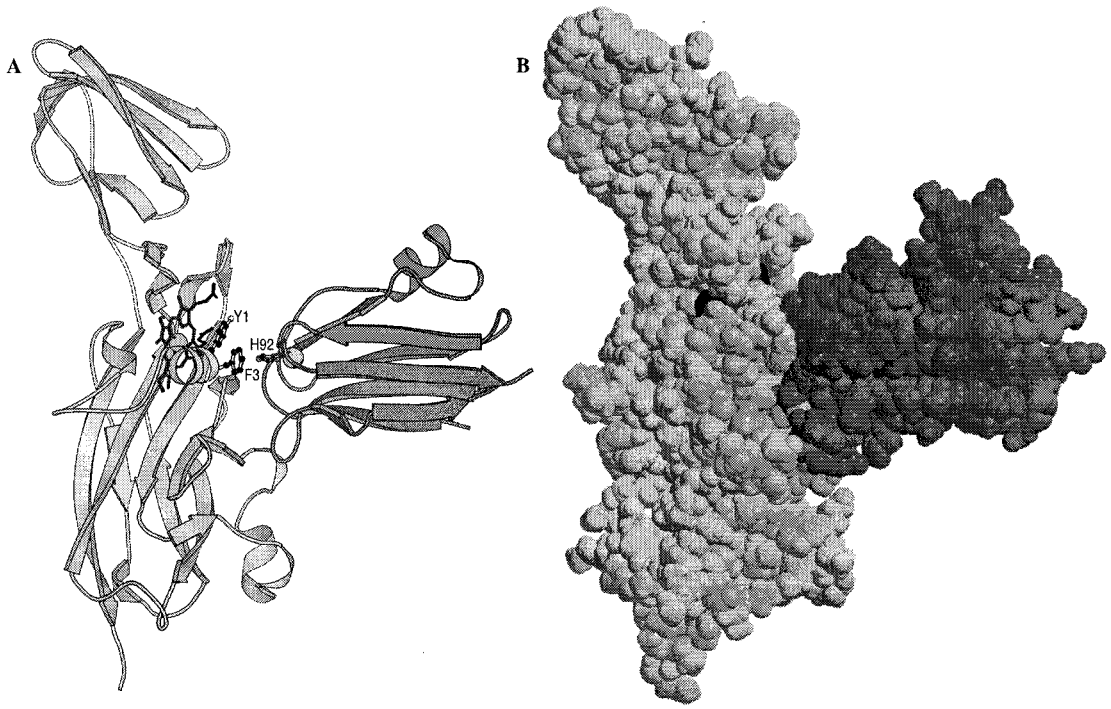

Figure 7. Representative structure of the Pc/cyt*f* complex from *P. laminosum* (A) in ribbon diagram and (B) in space-filling representations. In (A), His92 (Pc), Tyr1, and Phe3 (cyt*f*) are shown in ball-and-stick representation, and the heme is indicated in black.

not participate in the interface. Despite these differences, both systems are most likely to utilize His92 (H87) in the hydrophobic patch of Pc as the site of ET. In the *P. laminosum* complex, His92 makes contact with Phe3, while in the angiosperm complex, His87 makes contact with Tyr1, the sixth heme ligand of cyt*f*.[17] The surface area of the complex interface was calculated, using NACCESS,[71] to be 600−700 Å^2 of buried surface per protein. According to the classification of Lo Conte et al.,[72] this is a "standard-size" interface for a protein complex, and in such complexes only minor conformational changes between the free and complexed proteins are to be expected.

ET Complexes. Hervás et al. have proposed a hierarchy of three mechanisms of interprotein ET on the basis of the reactivity of Pc and cytochrome c_6 toward PSI.[73] The simplest is an oriented collisional mechanism with productive collisions yielding the ET reaction. In the second mechanism, protein collisions result in complex formation and subsequently ET. Complex formation followed by rearrangement of the interface, and subsequent ET completes this hierarchy. In the complex of spinach Pc and turnip cyt*f*, the third mechanism has been envisaged as follows: complementary charged surfaces produce an "electrostatic complex", allowing short-range hydrophobic forces to take effect and reorganize the interface to form the "reactive complex". The present work demonstrates that electrostatics play a minor role in the cyanobacterial complex, and therefore the molecular recognition is provided by the hydrophobic patch of Pc. There is no evidence for gross rearrangement of an encounter complex to a unique reactive complex. Therefore, in the context of the proposed hierarchy, the second model seems to apply.

The different reactivity of the two Pcs originates in their different surface and structural characteristics. While the β-sandwich structure is conserved among both proteins, the region from Ser60 (S58) to Leu64 (L62) extends further from the "north end" of spinach Pc, resulting in a more exposed loop. This prosthetic loop contains the upper acidic patch, Ser-Glu-Glu-Asp-Leu, which is relatively basic in *P. laminosum*, Ser-His-Ser-Gln-Leu. Furthermore, the "north end" of the *P. laminosum* molecule presents a larger and more compact hydrophobic patch than spinach Pc. From the analysis of hydrophobic interaction fields of type I copper proteins, De Rienzo et al. found that the cyanobacterial Pcs are grouped together with azurins and amicyanins and not with their angiosperm counterparts. On this basis they predicted different reaction mechanisms for the two Pc classes.[74]

Despite the functional similarity, it would appear that different mechanisms for ET from cyt*f* to Pc have evolved in different organisms. While a three-step mechanism based on the formation of an electrostatic complex is required in the angiosperm case, a two-step mechanism seems to be sufficient for the *P. laminosum* proteins. The present work demonstrates that hydrophobic interactions dominate in the latter, and the question arises as to whether a hydrophobic complex is capable of ET rates comparable to those of an electrostatic complex. Electrostatic attraction between the angiosperm proteins results in very fast reaction rates at low ionic strength. The electrostatic rate enhancement decreases rapidly, however, with increasing ionic strength,[15] and kinetic experiments demonstrate that the reaction rates for the *P. laminosum* system and the angiosperm system are similar at physiological ionic strength.[64] It is tempting to reconcile the hydrophobic nature of the Pc-cyt*f* complex in *P. laminosum* with the fact that the organism is a thermophile, which grows optimally at 45 °C, and thereby favors the hydrophobic effect.

(71) Hubbard, S. J.; Campbell, S. F.; Thornton, J. M. *J. Mol. Biol.* **1991**, *220*, 507−530.
(72) Lo Conte, L.; Chothia, C.; Janin, J. *J. Mol. Biol.* **1999**, *285*, 2177−2198.
(73) Hervás, M.; Navarro, J. A.; Díaz, A.; Bottin, H.; De la Rosa, M. A. *Biochemistry* **1995**, *34*, 11321−11326.
(74) De Rienzo, F.; Gabdoulline, R. R.; Menziani, M. C.; Wade, R. C. *Protein Sci.* **2000**, *9*, 1439−1454.

Acknowledgment. Dr. D. Bendall and Dr. C. Howe (University of Cambridge) are acknowledged for careful reading of the manuscript. We are grateful to Prof. L. Thöny-Meyer (ETH, Zurich) for kindly providing the plasmid, pEC86, which contains the cytochrome *c* maturation cassette. We thank Dr. J. Weigelt (Pharmacia-Upjohn, Stockholm) for measurements on the Varian Inova 800 and Dr. C. Erkelens (Leiden University) for his assistance with the NMR facilities. Financial support was provided by the Research Training Network 'TRANSIENT' in the Human Potential Program of the European Commission (HPRN-CT-1999-00095).

Supporting Information Available: Tables listing all residues which experience $|\Delta\delta_{bind}| \geq 0.05$ ($^1H^N$) or $|\Delta\delta_{bind}| \geq 0.07$ (^{15}N) in the complexes of *PCu* and *PCd* with ferrous cyt*f*; also included are those residues which demonstrate $|\delta_{PS}| \geq 0.05$ ($^1H^N$) or $|\Delta\delta_{PS}| \geq 0.07$ (^{15}N) (PDF). This material is available free of charge via the Internet at http://pubs.acs.org.

JA0112700